Letter

Flexible and superwettable bands as a platform toward sweat sampling and sensing

Xuecheng He, Tailin Xu, Zhen Gu, Wei Gao, Li-Ping Xu, Tingrui Pan, and Xueji Zhang

Anal. Chem., **Just Accepted Manuscript** • DOI: 10.1021/acs.analchem.8b05875 • Publication Date (Web): 18 Mar 2019

Flexible and Superwettable Bands as a Platform toward Sweat Sampling and Sensing

Xuecheng He,[†] Tailin Xu,[*,†] Zhen Gu,[†] Wei Gao,[‡] Li-Ping Xu,[*,†] Tingrui Pan,[§,∥] Xueji Zhang[*,†,#]

[†]Research Center for Bioengineering and Sensing Technology, Department of Chemistry and Biological Engineering, University of Science and Technology Beijing, Beijing 100083, P. R. China

[#]Beijing Advanced Innovation Center for Materials Genome Engineering, University of Science & Technology Beijing, 30 Xueyuan Road, Beijing 100083, P. R. China

[‡]Division of Engineering and Applied Science, California Institute of Technology, 1200 E California Boulevard, Pasadena, California 91125, United States

[§]Department of Biomedical Engineering, University of California, Davis, California 95616, United States

[∥]Shenzhen Institutes of Advanced Technology, Chinese Academy of Sciences, Shenzhen, Guangdong 518055, P. R. China

ABSTRACT: Wearable biosensors as a user-friendly measurement platform have become a rapidly growing field of interests due to their possibility in integrating traditional medical diagnostics and healthcare management into miniature lab-on-body analytic devices. This paper demonstrates a flexible and skin-mounted band that combines superhydrophobic-superhydrophilic microarrays with nanodendritic colorimetric biosensors toward in situ sweat sampling and analysis. Particularly, on the superwettable bands, the superhydrophobic background could confine microdroplets into superhydrophilic microwells. On-body investigations further reveal that the secreted sweat is repelled by the superhydrophobic silica coating and precisely collected and sampled onto the superhydrophilic micropatterns with negligible lateral spreading, which provides an independent "vessel" toward cellphone-based sweat biodetection (pH, chloride, glucose and calcium). Such wearable, superwettable band-based biosensors with improved interface controllability could significantly enhance epidemical sweat sampling in well-defined sites, holding a great promise for facile and noninvasive biofluids analysis.

Sweat has rapidly become one of appealing analytes owing to its easy epidermal availability without invasive procedure compared with other biofluids,[1,2] as well as abundant biomedical biomarkers related to health assessments and disease diagnoses such as metabolites,[3,4] electrolytes[5,6] and exogenous substances,[7,8] providing appreciative insight toward personalized medicine.[9] Considerable research towards diverse biosensors have been devoted for non-invasive and continuous sweat monitoring. Early sweat analysis rely on multistep operations involving manual fluidic collection (e.g. dripping or absorbing from the skin surface) and transfer to benchtop analytical devices.[10,11] Recently, soft and thin temporary tattoos, polymeric adhesive patches or fabric pads as flexible substrates in direct contact with skin are employed for *in situ* biosensing.[12-14] Additionally, microfluidic devices provide an alternative approach to address the collective issues by continuously guiding and extracting sweat into well-designed microchannels and performing analytics in an encapsulated micro-chamber.[15-19] Nevertheless, the sophisticated structures and connections of the conventional microfluidic devices in turn lead to complicated design and fabrication steps as well as increase the required sample amount and sampling time.[20]

Superwettable materials have proved to possess outstanding capability of on-demand fluidic manipulations, such as the directional drive of aqueous contents on a wettability gradient and spontaneous liquid transportation through the binary Janus membranes.[21-24] In particular, the superhydrophobic-superhydrophilic regions consist of miniature and compartmental micropatterns for the droplet-based interactions and reactions, in which the previous biomedical analytical technologies can be endowed with new possibilities such as high-throughput cell culture/array/screening.[25-29] Recently, tremendous efforts have been devoted to expansion of various

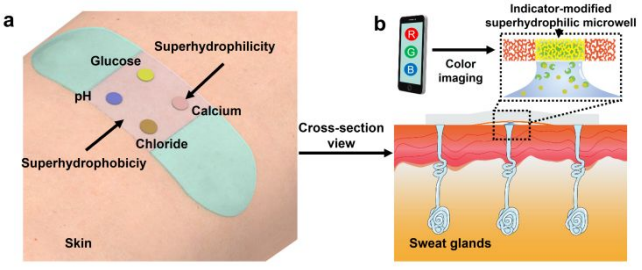

Figure 1. The concept of superwettable and flexible bands as a platform toward sweat sampling and monitoring. (a) Schematic of the band worn on a subject's epidermis for multiplex targets analysis. (b) Cross-section view of sweat pumped from subcutaneous sweat glands and precisely attracted on indicators-modified superhydrophilic microwells with a cellphone-assisted RGB screening module.

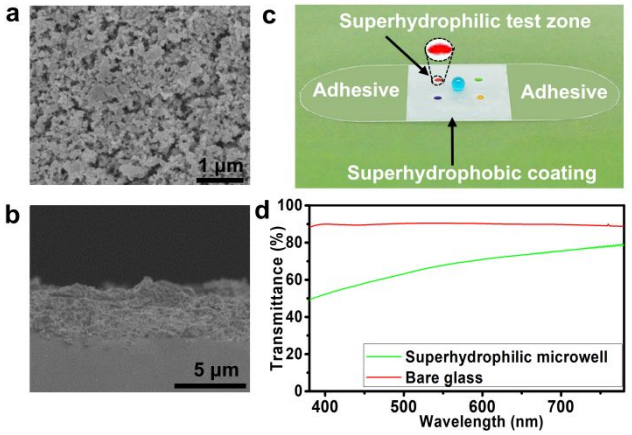

Figure 2. Physical characterization of the nanodendritic superwettable and flexible bands. (a) Top view and (b) side view of SEM imagines of the FAS-modified nanodendritic silica coating. (c) Structural layout of the superwettable band consisting of superhydrophobic coating, superhydrophilic microwells and adhesives layer. (d) UV-Vis-NIR transmission spectra of superhydrophilic microwell and bare glass.

biosensing approaches including colorimetric,[30-32] florescent[33,34] electrochemical[35,36] and surface-enhanced Raman scattering (SERS)[37,38] based on functionalized superhydrophilic microwells for detection of target biomolecules.

Herein, we fabricated the superwettable colorimetric sensing bands as a platform for *in situ* sweat sampling and analysis. The superwettable and wearable bands employ roll-to-roll coated nanodendritic silica onto a polyethylene terephthalate (PET) film as its superhydrophobic background, followed by shadow-masked oxygen plasma etching to define the superhydrophilic microwells. Driven by the extreme wettability gradient, the continuously generated perspiration on human skin tends to be collected into the superhydrophilic microwells, where colorimetric detection of sweat can be achieved with a cellphone-based image recognition. This work may provide a promising route for the development of facile and wearable point-of-care diagnostic devices.

As schematically demonstrated in **Figure 1,** the superwettable sweat assay band mainly consists of three compositions: (1) an epidermis-compatible adhesive layer that can provide temporal yet sufficient physical attachment to human skin, (2) an indicators-embedded superhydrophilic microarray for well-defined sweat collecting and multiplexed sensing, (3) a superhydrophobic silica background for preventing sweat from spreading and concentrating the secreted biofluid in the superhydrophilic spots. The whole device is arranged and fabricated on a soft and flexible PET substrate, which enables conformal contact with the curved epidermal contours. The core sensing elements lays on the functionalized superhydrophilic microarray, of which the design principle is described in **Figure 1b**. Schematically, the sweat continuously secreted from subcutaneous glands can be preferably absorbed onto the indicators-modified superhydrophilic microwells due to the strong capillary forces from the porous microstructures, inducing the downstream colorimetrical reaction that can be transformed into a concentration-dependent color feedback by a portable cellphone.

The superwettable sweat bands with superhydrophobic-superhydrophilic microarrays were fabricated by combining the roll-to-roll coating of the nanoparticle suspension and the

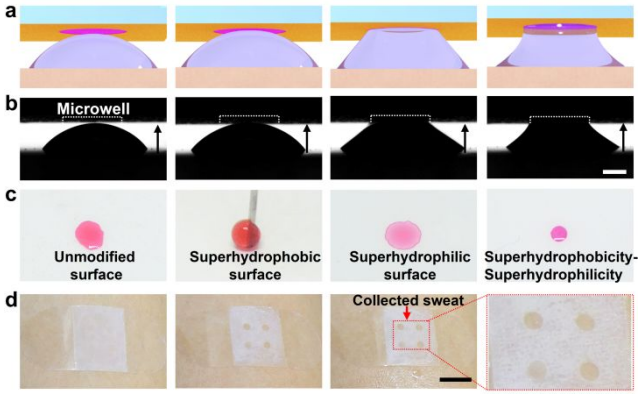

Figure 3. Sweat collection profiles on superwettable bands. Schematic (a) and corresponding microscopic images (b) of simulated sweat harvest via gradually lifting the glass plate with 1.0 μL water droplet (mimicking tiny sweat on skin) to approach the upper band. Scale bar: 500 μm. (c) Artificial sweat droplet on different wettability displays its unique capacity of anchoring microdroplets in superhydrophilic microwell. (d) On-body sweat collection in the pre-designed microwells during continuous exercise. Scale bar: 1 cm.

shadow-masked oxygen plasma etching techniques, which is detailed in **Supporting Information**. In brief, the superhydrophobic silica suspension was prepared and coated onto PET film after natural evaporation.[39] As demonstrated in **Figure 2a and 2b**, the topographically roughened silica layer comprises physically connected dendritic-like network of random spherical particles in diameter ranging from 20 to 40 nm with an average thickness of ~5 μm. Dye-labelled droplets present dramatic differences on the bands as shown in **Figure 2c**. The microdroplets on the silica coating were quasi-spherical, suggesting the superhydrophobicity. In contrast, water droplets in microwells were almost flattened, indicating the superhydrophilicity of such plasma-etched microarray. In addition, the superwettable bands exhibited fine optical transparency with less than 30% reduction compared to bare glass as shown in **Figure 2d**, which was beneficial for accessible colorimetric readouts.

The sweat extract processes were simulated schematically and experimentally by designing a simple microdroplet-capturing model as demonstrated in **Figure 3a** and **3b**. Briefly, a glass slip slide with 1.0 μL water droplet (mimicking tiny sweat on skin) and the superwettable band were first placed face-to-face. Upon slightly lifting the bottom glass plate towards approach the upper band, the microdroplet precisely grabbed onto the pre-defined microwell, undergoing appearance altering from circular arch to a thin neck next to the superwettable band. As demonstrated in **Figure S1**, the collected sample displayed an increase in volume from 0.42, 0.70, 0.84, 1.57 to 1.99 μL along with the size of the microwells ranging from 0.5 to 2.5 mm, showing good agreement with the porous superhydrophilic microwells model within size-dependent capillary forces.[40] Therefore, the amount of sample solution can be on-demand regulated by adjusting the dimensions of the microwells accordingly.

To better understand the relationship between the interfacial property of the band and microdroplet behaviors, we compared our superwettable bands with control groups including unmodified, superhydrophilic, and superhydrophobic surface as shown in **Figure 3c**. Artificial sweat droplets irregularly spread

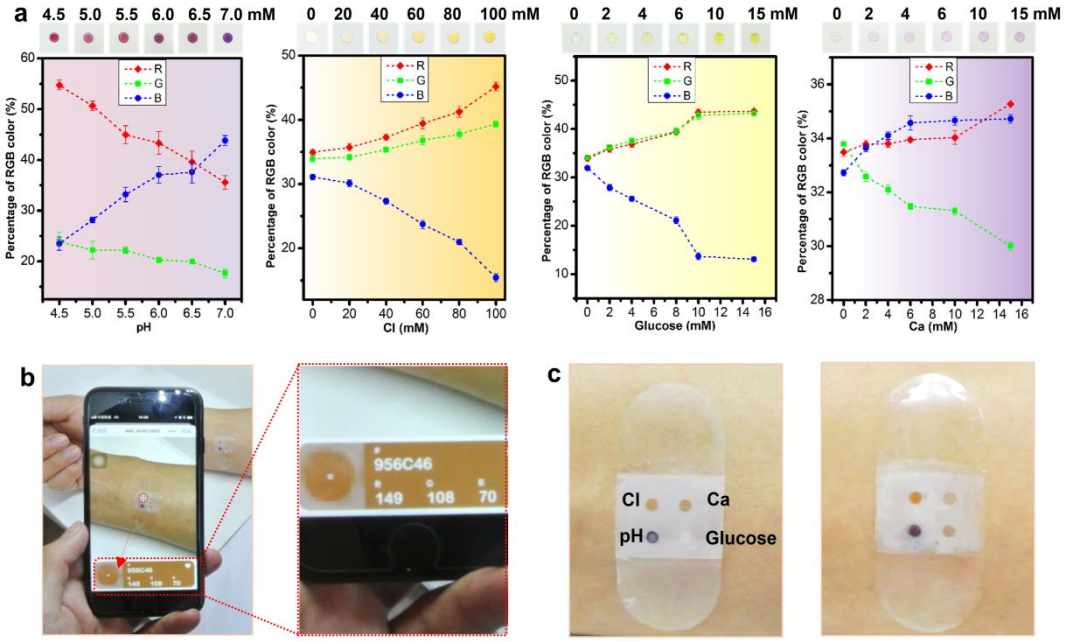

Figure 4. Superwettable bands toward multiplex sweat biosensing. (a) Calibration plots of normalized %RGB value versus pH, chloride, glucose and calcium concentration for quantitative perspiration analysis (n = 3, error bars represent the standard deviation). Each colored dots in the graph vertically matches microdroplets of gradient concentration above. (b) App-assisted cellphone as screening module capable of adjusting the viewing position (white cross) to the targeted sites on the bands to verify RGB (red, green, and blue) information. (c) Color contrast of superhydrophilic microarray before (left) and after (right) raw sweat secretion.

out on superhydrophilic and hydrophilic surface with a relatively large infiltration range, or repelled by the superhydrophobic substrate. In contrast, the superwettable bands displayed the unique capacity of immobilizing microdroplet in well-defined superhydrophilic spot. **Figure 3d** illustrates the epidemical sweat sampling investigation. A subject wearing the superwettable band was commanded to exercise for several minutes to ensure a visible amount of sweat. The secreted sweat well-defined collected in the superhydrophilic spots, and the superhydrophilic microwells presented a transparent state after wetted by the sweat. In contrast, the superhydrophobic area was opaque and almost dry. Visual observation showing the microwells totally occupied and wetted by the sweat can ensure the chamber was full before downstream detection. Such decentralized sweat collecting profile precisely defines the analytical site, hindering the area located outside the biodetection access from any exposure to moisture when conformal contact on sweaty epidermis, which is particularly essential for the circuit elements of electrochemical sensors to ensure the electrical insulation and waterproof.

Picturing color changes of the targets microdroplets and converting them into digital feedback were investigated in **Figure 4** by cellphone-assisted operation. The standardized %RGB versus multivariate targets abundance were plotted in **Figure 4a,** which were recorded by moving the viewing position (white cross) to the targeted sites of assay zone to extract individual R, G, B and convert into %RGB format via an open-source color analytical App (Color Pick®) shown in **Figure 4b**. For pH determination, as revealed in **Figure 4a**, microdroplets with rising pH values from 4.5 to 7.0 with a resolution of 0.5 resulted in a considerably reduced R percentage from 55 % to 36 %, while an increased B percentage from 23% to 44%, consistent with the appreciable color alteration from red to purple. For chloride and glucose targets, the welled microdroplet gradually turned into yellow as concentration increased from 0, 20, 40, 60, 80 to 100 mM and from 0, 2, 4, 6, 10 to 15 mM, respectively, accompanied with rising red and green proportion (The combinatorial color of yellow). Similarly, calcium analytes ranging from 0, 2, 4, 6, 10, 15 mM with deeper purple lead to higher red and blue percentages (The combinatorial color of purple). These calibration plots are in fine accordance with trichromatic theory, bridging the analytes abundance and digitally processed color data for semi-quantitative analytical work.

In the end, the superwettable bands were adhered onto the wrist of a healthy volunteer, followed by continuous exercise to evaluate the sensing performance of raw sweat using the standardized curves. **Figure 4c** demonstrates that the microchip performed as anticipated, successfully collecting sweat within the indicator-modified microarray without any detachment. Additionally, the generated perspiration rationally changed the intrinsic color of each assay zone at different degrees: the pH region underwent a color altering from blue to light fuchsia and chloride turned the colorimetric reagent from yellow to deep orange. By visual comparison of corresponding calibrations, it can be roughly perceived that the sweat is weakly acidic with pH between 6.5-7.0 and chloride concentration around 100 mM. However, the calcium and glucose targets remained almost colorless statues, indicating their trace content. These results are well compatible with the reported physiological ranges in normal human beings.[41] Therefore, the portable cellphone screening mode integrated with standardized plots is helpful for semi-quantitatively interpreting targets concentrations, exhibiting favorable potential toward practical application.

In conclusion, a flexible and superwettable band for continuous sweat collection and analytic has been reported as a healthcare monitoring platform in this paper. Taking advantages of the superwettability toward effectively harvesting moisture the bands illustrate promising potential to

develop wearable devices for sweat collection and biosensing. By embedding colorimetric-indicators in the superhydrophilic test zones, we have successfully achieved a proof-of-concept analysis of sweat by combining a mobile cellphone. Despite of some drawbacks, for example, the bands fail to achieve real-time sweat monitoring and reveal the sweat rate effect. These items are expected to be overcome by armed with advanced sensing technology in future efforts. The intrinsically simple, low-cost property of the bands can facilitate their potential commercialized distribution in emerging personal healthcare and clinical monitoring field.

ASSOCIATED CONTENT

Supporting Information

The Supporting Information is available free of charge on the ACS Publications website.

Detailed materials, instruments, experiment section and additional figures (PDF).

AUTHOR INFORMATION

Corresponding Author

*E-mail: xutailin@ustb.edu.cn.
*E-mail: xuliping@ustb.edu.cn.
*E-mail: zhangxueji@ustb.edu.cn.

Notes

The authors declare no competing financial interest.

ACKNOWLEDGMENT

We acknowledge funding from National Natural Science Foundation of China (21804007, 21890740, 21890742), Beijing Natural Science Foundation (2184109), Fundamental Research Funds for Central Universities (FRF-TP-17-066A1), National Postdoctoral Innovative Talents Support Program of China (BX20180036), and Program for Guangdong Introducing Innovative and Entrepreneurial Teams (2016ZT06D631), and the Shenzhen Fundamental Research Program (JCYJ20170413164102261).

Reference

(1) Yang, Y.; Gao, W. *Chem. Soc. Rev.* **2018**, DOI: 10.1039/C7CS00730.
(2) Choi, J.; Ghaffari, R.; Baker, L. B. *Sci. Adv.* **2018**, *4*, eaar3921.
(3) Lee, H.; Choi, T. K.; Lee, Y. B.; Cho, H. R.; Ghaffari, R.; Wang, L.; Choi, H. J.; Chung, T. D.; Lu, N.; Hyeon, T.; Choi, S. H.; Kim, D. H. *Nat. Nanotechnol.* **2016**, *11*, 566-572.
(4) Parlak, O.; Keene, S. T.; Marais, A.; Curto, V. F.; Salleo, A. *Sci. Adv.* **2018**, *4*, eaar2904.
(5) Gao, W.; Emaminejad, S.; Nyein, H. Y. Y.; Challa, S.; Chen, K.; Peck, A.; Fahad, H. M.; Ota, H.; Shiraki, H.; Kiriya, D.; Lien, D. H.; Brooks, G. A.; Davis, R. W.; Javey. *Nature* **2016**, *529*, 509-514.
(6) Emaminejad, S.; Gao, W.; Wu, E.; Davies, Z. A.; Yin Yin Nyein, H.; Challa, S.; Ryan, S. P.; Fahad, H. M.; Chen, K.; Shahpar, Z.; Talebi, S.; Milla, C.; Javey, A.; Davis, R. W. *Proc. Natl. Acad. Sci. U.S.A.* **2017**, *114*, 4625-4630.
(7) Tai, L. C.; Gao, W.; Chao, M.; Bariya, M.; Ngo, Q. P.; Shahpar, Z.; Nyein, H. Y. Y.; Park, H.; Sun, J.; Jung, Y.; Wu, E.; Fahad, H. M.; Lien, D. H.; Ota, H.; Cho, G.; Javey, A. *Adv. Mater.* **2018**, *30*, e1707442.
(8) Kim, J.; Jeerapan, I.; Imani, S.; Cho, T. N.; Bandodkar, A.; Cinti, S.; Mercier, P. P.; Wang, J. *ACS Sens.* **2016**, *1*, 1011-1019.
(9) Heikenfeld, J.; Jajack, A.; Rogers, J.; Gutruf, P.; Tian, L.; Pan, T.; Li, R.; Khine, M.; Kim, J.; Wang, J.; Kim, J. *Lab Chip* **2018**, *18*, 217-248.
(10) Eng, W.; LeGrys, V. A.; Schechter, M. S.; Laughon, M. M.; Barker, P. M. *Pediatr. Pulmonol.* **2005**, *40*, 64-67.
(11) Desax, M. C.; Ammann, R. A.; Hammer, J.; Schoeni, M. H.; Barben, J.; Swiss Paediatric Respiratory Research, G. *Eur. J. Pediatr.* **2008**, *167*, 299-304.
(12) Wang, S.; Wu, Y.; Gu, Y.; Li, T.; Luo, H.; Li, L. H.; Bai, Y.; Li, L.; Liu, L.; Cao, Y.; Ding, H.; Zhang, T. *Anal. Chem.* **2017**, *89*, 10224-10231.
(13) Gao, W.; Nyein, H. Y. Y.; Shahpar, Z.; Fahad, H. M.; Chen, K.; Emaminejad, S.; Gao, Y. J.; Tai, L. C.; Ota, H.; Wu, E.; Bullock, J.; Zeng, Y. P.; Lien, D. H.; Javey, A. *ACS Sens.* **2016**, *1*, 866-874.
(14) Wang, L.; Wang, L.; Zhang, Y.; Pan, J.; Li, S.; Sun, X.; Zhang, B.; Peng, H. *Adv. Funct. Mater.* **2018**, *28*, 1804456.
(15) Nyein, H. Y. Y.; Tai, L. C.; Ngo, Q. P.; Chao, M.; Zhang, G. B.; Gao, W.; Bariya, M.; Bullock, J.; Kim, H.; Fahad, H. M.; Javey, A. *ACS Sens.* **2018**, *3*, 944-952.
(16) Koh, A.; Kang, D.; Xue, Y.; Lee, S.; Pielak, R. M.; Kim, J.; Hwang, T.; Min, S.; Banks, A.; Bastien, P.; Manco, M. C.; Wang, L.; Ammann, K. R.; Jang, K. I.; Won, P.; Han, S.; Ghaffari, R.; Paik, U.; Slepian, M. J.; Balooch, G., Huang, Y., Rogers, J. A. *Sci. Transl. Med.* **2016**, *8*, 366ra165.
(17) Martin, A.; Kim, J.; Kurniawan, J. F.; Sempionatto, J. R.; Moreto, J. R.; Tang, G.; Campbell, A. S.; Shin, A.; Lee, M. Y.; Liu, X.; Wang, J. *ACS Sens.* **2017**, *2*, 1860-1868.
(18) Sekine, Y.; Kim, S. B.; Zhang, Y.; Bandodkar, A. J.; Xu, S.; Choi, J.; Irie, M.; Ray, T. R.; Kohli, P.; Kozai, N.; Sugita, T.; Wu, Y.; Lee, K.; Lee, K. T.; Ghaffari, R.; Rogers, J. A. *Lab Chip* **2018**, *18*, 2178-2186.
(19) Choi, J.; Kang, D.; Han, S.; Kim, S. B.; Rogers, J. A. *Adv. Healthc. Mater.* **2017**, *6*, 1601355.
(20) Yang, Y.; Xing, S.; Fang, Z.; Li, R.; Koo, H.; Pan, T. *Lab Chip* **2017**, *17*, 926-935.
(21) Zheng, Y.; Bai, H.; Huang, Z.; Tian, X.; Nie, F. Q.; Zhao, Y.; Zhai, J.; Jiang, L. *Nature* **2010**, *463*, 640-643.
(22) Xing, S.; Jiang, J.; Pan, T. *Lab Chip* **2013**, *13*, 1937-1947.
(23) Zhu, P.; Wang, L. *Lab Chip* **2016**, *17*, 34-75.
(24) Zhao, Y.; Wang, H.; Zhou, H.; Lin, T. *Small* **2017**, *13*, 1601070.
(25) Neto, A. I.; Correia, C. R.; Custodio, C. A.; Mano, J. F. *Adv. Funct. Mater.* **2014**, *24*, 5096-5103.
(26) Shi, W.; Xu, T.; Xu, L. P.; Chen, Y.; Wen, Y.; Zhang, X.; Wang, S. *Nanoscale* **2016**, *8*, 18612-18615.
(27) Ueda, E.; Levkin, P. A. *Adv. Mater.* **2013**, *25*, 1234-1247.
(28) Garcia-Cordero, J. L.; Fan, Z. H. *Lab Chip* **2017**, *17*, 2150-2166.
(29) Feng, W.; Ueda, E.; Levkin, P. A. *Adv. Mater.* **2018**, *30*, 1706111.
(30) Han, H.; Lee, J. S.; Kim, H.; Shin, S.; Lee, J.; Kim, J.; Hou, X.; Cho, S. W.; Seo, J.; Lee, T. *ACS Nano* **2018**, *12*, 932-941.
(31) Hou, J.; Zhang, H.; Yang, Q.; Li, M.; Jiang, L.; Song, Y. *Small* **2015**, *11*, 2738-2742.
(32) He, X.; Xu, T.; Gao, W.; Xu, L. P.; Pan, T.; Zhang, X. *Anal. Chem.* **2018**, *90*, 14105-14110.
(33) Huang, Y.; Li, F.; Qin, M.; Jiang, L.; Song, Y. *Angew. Chem. Int. Ed.* **2013**, *52*, 7296-7729.
(34) Xu, L. P.; Chen, Y.; Yang, G.; Shi, W.; Dai, B.; Li, G.; Cao, Y.; Wen, Y.; Zhang, X.; Wang, S. *Adv. Mater.* **2015**, *27*, 6878-6884.
(35) Zhang, H.; Oellers, T.; Feng, W.; Abdulazim, T.; Saw, E. N.; Ludwig, A.; Levkin, P. A.; Plumeré, N. *Anal. Chem.* **2017**, *89*, 5832-5839.
(36) Xu, T.; Song, Y.; Gao, W.; Wu, T.; Xu, L.-P.; Zhang, X.; Wang, S. *ACS Sens.* **2018**, *3*, 72-78.
(37) Li, H. Z.; Yang, Q.; Hou, J.; Li, Y. A.; Li, M. Z.; Song, Y. L. *Adv. Funct. Mater.* **2018**, *28*, 1800448.
(38) Song, Y.; Xu, T.; Xu, L.-P.; Zhang, X. *Nanoscale* **2018**, *10*, 20990-20994.
(39) Wang, P.; Chen, M.; Han, H.; Fan, X.; Liu, Q.; Wang, J. *J. Mater. Chem. A* **2016**, *4*, 7869-7874.
(40) Xu, T.; Shi, W.; Huang, J.; Song, Y.; Zhang, F.; Xu, L. P.; Zhang, X.; Wang, S. *ACS Nano* **2017**, *11*, 621-626.
(41) Bariya, M.; Nyein, H. Y. Y.; Javey, A. *Nat. Electron.* **2018**, *1*, 160-171.

For TOC only

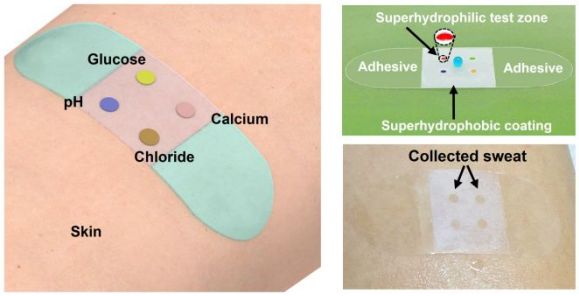
Glucose
pH
Calcium
Chloride
Skin
Superhydrophilic test zone
Adhesive
Adhesive
Superhydrophobic coating
Collected sweat